Supporting Information

Nitrogen Doped Biocompatible Carbon Dot as a Fluorescent Probe for STORM Nanoscopy

*Navneet C. Verma, Chethana Rao and Chayan K. Nandi**

School of Basic Sciences, Indian Institute of Technology Mandi, Mandi, Himachal Pradesh 175001, India.

*Corresponding Author : chayan@iitmandi.ac.in

Experimental Procedures

UV-Vis Absorption and steady state fluorescence spectroscopy

The UV-Vis absorption spectra were recorded using Shimadzu UV-Vis 2450 spectrophotometer. The spectra were collected using a quartz cuvette having 10 mm path length and 1 ml volume. All the measurements were repeated at least three times. Steady state fluorescence was measured using Horiba Fluorolog-3 spectrofluorometer. The fluorescence was measured in 1 ml quartz cuvette.

Transmission Electron Microscope (TEM):

The particle size and dispersity of the synthesized nanoparticles were performed using a TECNAI G2 200 kV TEM (FEI, Electron Optics) electron microscope with 200 kV input voltage. TEM grids were prepared by placing 5 µL diluted and well sonicated sample solution on a carbon coated copper grid and evaporated the solution at room temperature completely. Precautions were taken to avoid contamination from various sources like dust particles and glassware.

Fourier Transform Infrared Spectroscopy (FTIR):

FTIR spectra of CD were measured using a Perkin-Elmer FTIR spectrophotometer equipped with a horizontal attenuated total reflectance (ATR) accessory containing a zinc selenide crystal and operating at 4 cm^{-1} resolution. The use of the spectral subtraction provided reliable and reproducible results. KBr pellets have been used as a reference and for the baseline correction.

Atomic Force Microscopy (AFM):

AFM analysis of the synthesized nanoparticles for particle size determination was carried out using a Digital Instruments Bruker AFM. Standard Veeco tapping mode silicon probes were used for scanning the samples. Typically, aqueous suspensions of CD samples were dried on silicon substrate for 3h. Once dried, samples were placed on the AFM and scanned. Pertinent scanning parameters were as follows:

Resonant frequency (probe): 60-80 kHz; Tip velocity for all measurements are: (4μm/s for 2μm), (15μm/s for 5μm), (30μm/s for 10μm). Aspect ratio: 1:1; Resolution: 512 samples/line, 256 lines.

X-ray photoelectron spectroscopy (XPS):

X-ray Photo-Electron Spectroscopy (XPS) with Auger Electron Spectroscopy (AES) module PHI 5000 Versa Prob II,FEI Inc. and C60 sputter gun has been used for characterization and scanning the spectra from C1s to O1s region. Al Kα X-ray radiation was used as the source for excitation (1486.8 eV, 500 mm). Samples are loaded on copper strips, and surface adherence done through double sided adhesive tape. Scanning has been done for combined and independently for C1s, N1s and O1s at their specific binding energy.

Cytotoxicity assay (MTT)

The in-vitro cytotoxicity was measured using a standard MTT assay. HeLa cell were seeded into 96-well cell culture plate at 10^4/well and then incubated for 24 h at 37°C under 5% CO_2. The cells were incubated with varying concentration of CD for 72 h, followed by 1 hour incubation with the MTT reagent. The optical density of the sample was recorded using multimode plate reader (TECAN).

Single molecule time trace, photon counts and localization based superresolution:

CD and Cy3 dye were spin coated on a clean glass slide to collect single molecule time traces. The diffraction limited spots produced due to single molecule blinking, under laser excitation were observed using 60x oil immersion Nikon TIRF objective mounted on a custom build inverted optical microscope and 1.5x extra magnification in the optical path. A 532 nm diode laser with 50mW power was used for excitation. A 532nm high pass Dichoric along with 580/70 nm optical filter (AHF Analysentechnik) was used to separate the excitation and emission light. Andor EMCCD iXon Ultra was used to record the single molecule photon events at the readout rate of 17 MHz and exposure time of 5-100ms. The time trajectories were recorded and analyzed using the Andor Solis Software. The

incident photons were converted to electrons and subsequent to digital counts by the EMCCD camera. The signals were recorded using single photon counting mode of iXon EMCCD which provides minimum noise floor for acquisition. A home built Matlab program was used to separate single molecule event by taking group of 3x3 pixels covering whole diffraction limited spots with each pixel size equal to 177nm. Other spots with less than one pixel distance were removed from the study. The number of photons ware calculated by the maximum counts, above the mean value of the noise floor. The blinking events were counted by fitting the events having fluorescence fluctuations more than 5 times of the background standard deviation. For the movies, recorded under kinetic mode of EMCCD, time/frame trajectories of the counts/intensity at a given pixel, were obtained for the provided exposure time. These time trajectories were saved for further analysis. The image area of only 128x128 pixels was taken from the total 512x512 pixels of the whole sensor of EMCCD. A small area of the sensor was used for faster image acquisition using crop-sensor mode of iXon EMCCD. Thus, we used the total image area of 128x128 pixels.

For the localization experiments, same dichroic and filter combination were used. An image projection lens was used to project image at the sensor of EMCCD. The number of photons per pixel was determined using EMCCD photon counting mode. Background was calculated from the image area where no molecule was present during the measurement time. The mean value of this background was subtracted from the original trajectory to obtain a background free signal. For further correction, background signal (after complete photobleaching) were also set to zero level. GDSC ImageJ Plugins were used for optical reconstruction. (Code available on http://www.sussex.ac.uk/gdsc/intranet/microscopy/imagej/smlm plugins). For the localization of single CD, all photons emitted by the CD were used instead of single blinking event. We have also performed the experiment with cyanine dye molecule and compared the results. The localization was performed by SMLM-GDSC plugin which calculate the theoretical limit (precision) for fitting the signal (number of photons) and the XY coordinates (localisation). The background noise is estimated by the PEAK FIT plugin during the fitting process using a global noise estimate per frame. A camera with 16 μm pixel

size and a 60x objective with 1.5 magnification (pitch of 16000/60=177.78 nm) was used. Exposure time of 50ms, wavelength of 570 nm and 1.40 numerical aperture of the objective was chosen. The standard deviation of the Gaussian approximation to the PSF was calculated by the following formula.

$SD=p\times1.323\times\lambda/2\pi NA$

Where λ is the wavelength (in nm), NA is the Numerical Aperture and p is the proportionality factor. A value of p=1 gives the theoretical lower bounds on the peak width. However due to the limitations of the microscope optics and stage drift, the fitted width is often wider than this limit. The value of p was taken 1.52. Data was processed by fitting Gaussian functions to individual molecule fluorescence blinking events. The minimum FWHM of the structures were obtained by the measurement along different parts of the same super resolved structure. The multiple measurements were performed to find the standard deviation of the result.

The blinking rate of a fluorophore depends on the laser power. If the laser power is high on-off rate will be higher. To capture the blinking events of the fluorophore, the camera frame rate must be synchronized with the time scale of the blinking events. If the frame rate is lower than the switching speed of the fluorophore, there is a chance to miss a significant amount of the events for low switching rate and in opposite at high camera speed, extra repeated frames can be imaged with no use of them.[1] The EMCCD used in this experiment worked on 17MHz readout rate with 5-50ms exposure times which provides around 200-20s^{-1} frame rate for the camera. The observed on time of the carbon dots comes in the range of 0.01-10.00s with 20mw laser power, which can be easily detected at these camera frame rates. Here, we have improved the environmental condition to increase the switching cycle of the carbon dots and optimized its imaging conditions by the addition of methyl viologen and with optimum laser power. To capture the blinking events of the fluorophores attached with nanostructures, the camera frame rate was synchronized with the time scale of the blinking events. Even for some of the non-blinking or slowly blinking fluorophore, there may be over waited localizations can come in a certain part of the images and can create the difficulty in the actual size determination of the sample. There are

several other reasons which can cause the artifacts in the localization based microscopy, one of them is the nonrobust switching which leads to the detection of a lower number of fluorophores than actual and the resultant image contains fewer details.[2] On the other hand, in the lack of improper blinking the background signal or multiple emitters can be detected as a single fluorophore.[3] In the case of CD, the blinking rate and camera frame rate were synchronized. In general, in localization based microscopy one cannot achieve the predicted theoretical value of resolution due to the linker length and flexibility, as in the case of immunostaining, or due to imaging limitation such as the drift. In that case, the experimental localization precision is determined by measuring multiple localizations of the same emitter and calculating the standard deviation of the Gaussian distribution of these localizations, but this method fails for very densely tagged structures where well-separated single emitters are not available. If for any reason more than one fluorophore out of all, present within a two-dimensional diffraction-limited area, when the fluorophore is in the on state, the overlapping point-spread-functions (PSFs) are generated resulting in false multiple-fluorophore localizations. It also fails if any given single molecule is not localized in multiple frames. In above-mentioned cases, the determination of the spatial resolution of a well-defined structure is an option.[3] It is well known that the theoretical upper limit of the localization precision, primarily depends on the fitting performance and therefore, mainly on the number of photons detected per localized spot. Since the appropriate laser power controls the lifetime of a fluorophore's on-state, the areas having a higher fluorophore density require higher irradiation intensities to ensure efficient transfer of fluorophores to the nonfluorescent or bleached off-state. The information theory tells that the required density of fluorescent probes has to be sufficiently high to satisfy the Nyquist–Shannon sampling theorem. The density of fluorophores and simultaneously the size of the fluorescent probes control the achievable structural resolution, therefore, the efficient proper labeling procedure and small structures are crucial for artifact-free localization microscopy.

Results and Discussion

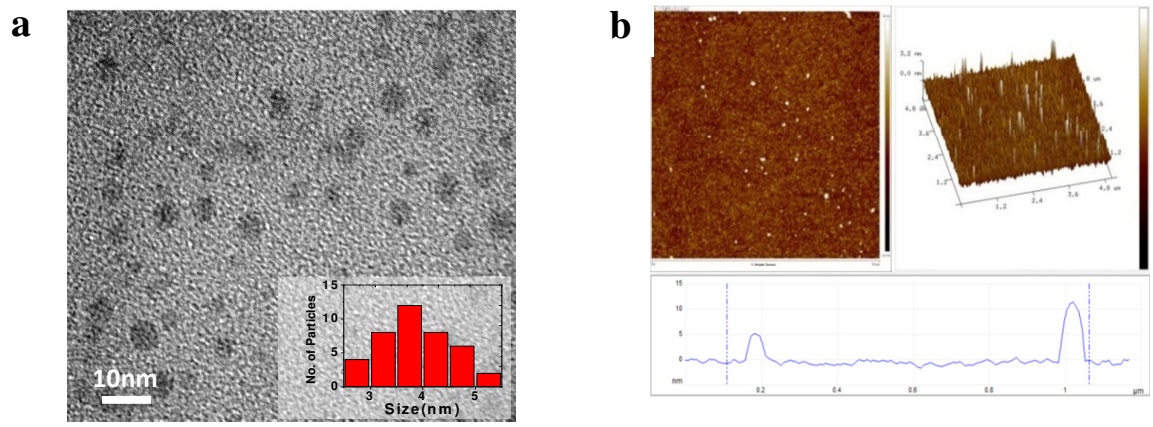

Figure S1. (a) Transmission electron microscopy (TEM) of the CD. Inset shows the mean particle size of 3.8nm by the statistical analysis of all the particles shown in the image. (b) Atomic force microscopic image of the CD shows the similar size distribution as TEM image. Homogeneous size was observed in both the cases.

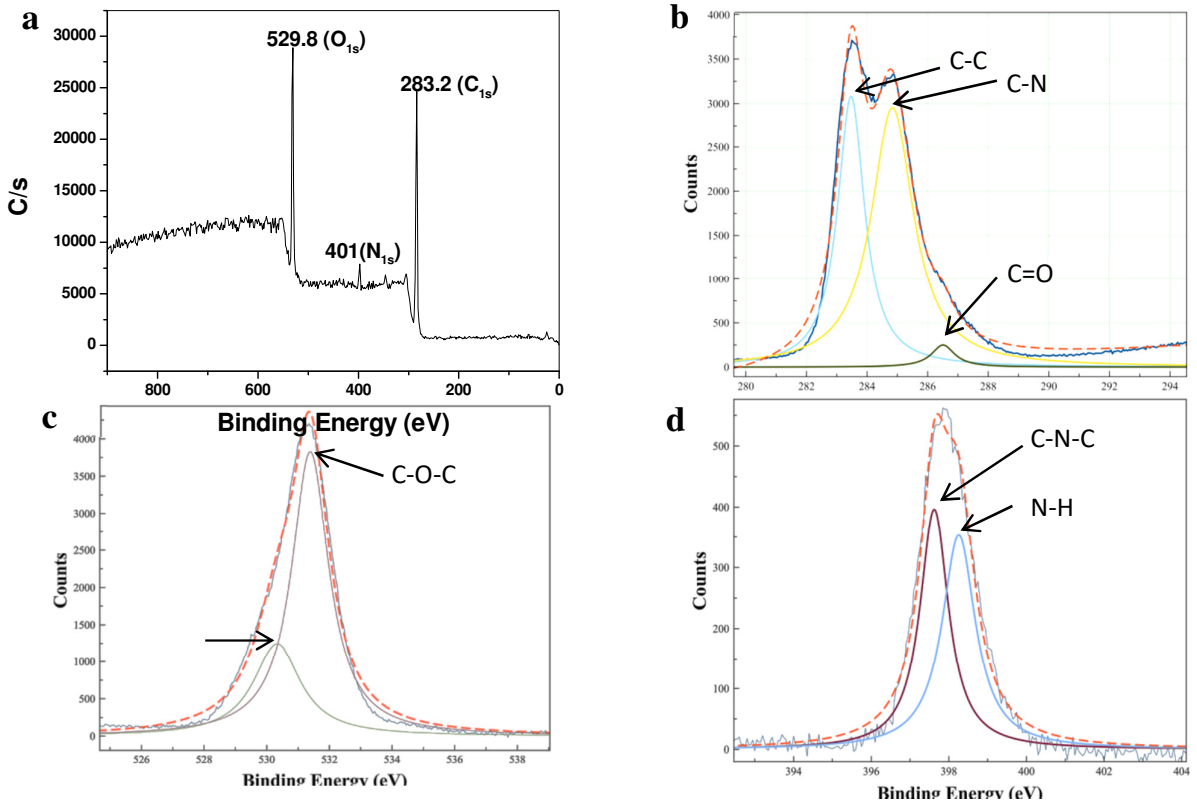

Figure S2. (a) XPS spectrum of the as synthesized CD shows three major peaks of C1s, O1s and N1s respectively. (b), (c) and (d) showed the high resolution C1s, O1s and N1s spectra.

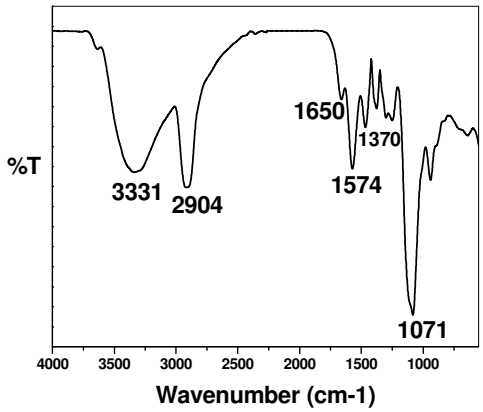

Figure S3. FTIR spectrum confirms the presence of COOH, NH_2 and OH functional groups on the surface of CD.

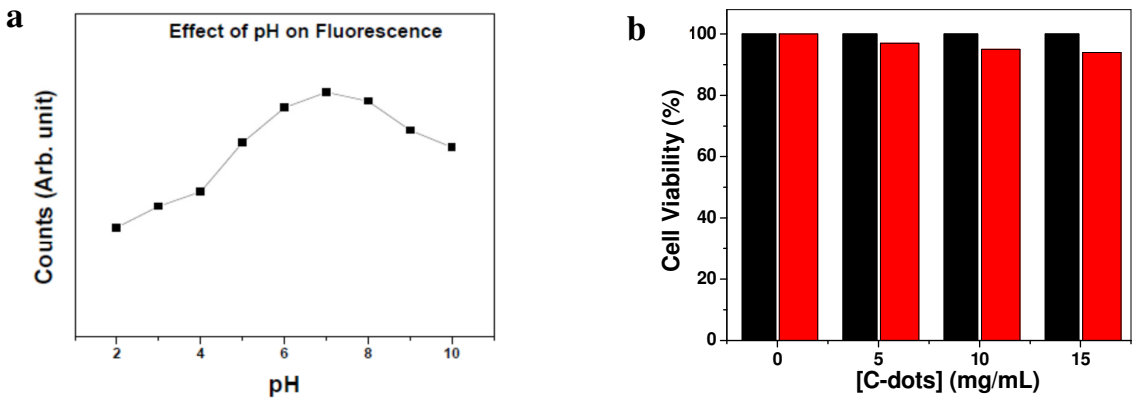

Figure S4. Effect of pH on the fluorescence emission properties of CD. (a) Maximum fluorescence intensity is observed around at around pH =7.0 (b) Measurement of cell viability by MTT assay. The CD is almost nontoxic even in very high concentration of CD.

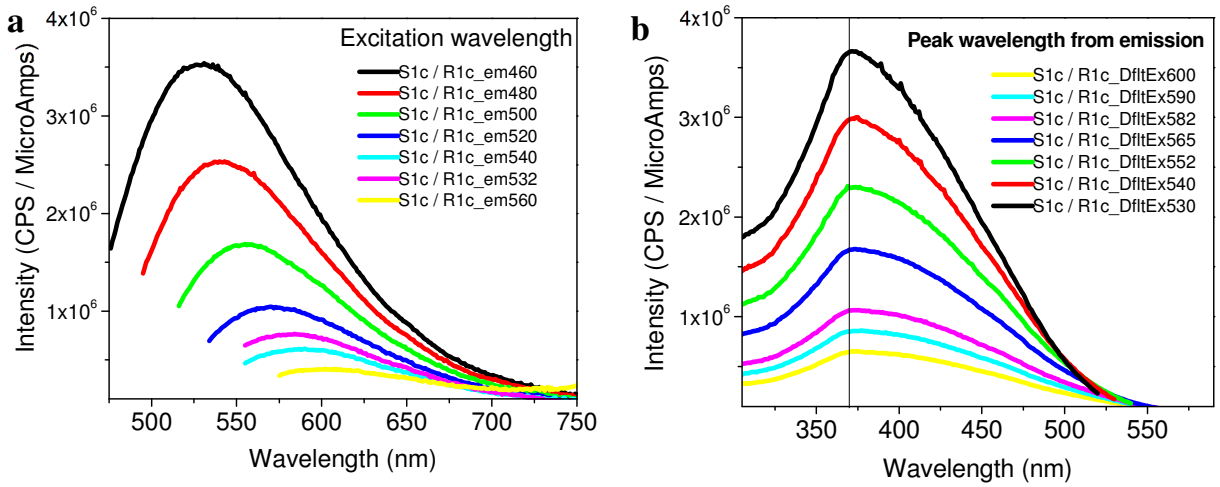

Figure S5. (a) Fluorescence emission spectra of CD shows excitation dependent behavior, i.e. the emission peak shifts after changing the excitation position. The excitation wavelength shown in legend and **(b)** the excitation spectra corresponding to each emission peak value taken from the fluorescence emission spectrum .

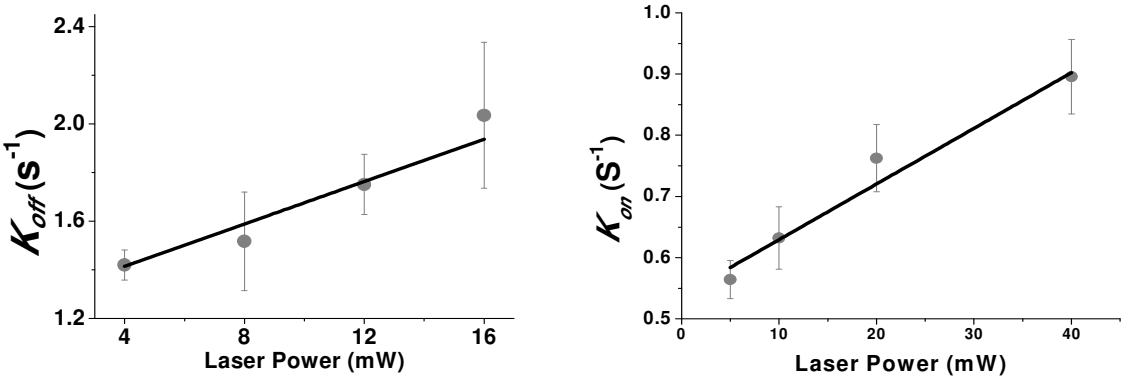

Figure S6. Laser power dependent on–off rate. The data shows the linear dependency of the rate constants K_{off} and K_{on} in both the cases. The error bar represents the deviation in the mean value of the different measurements.

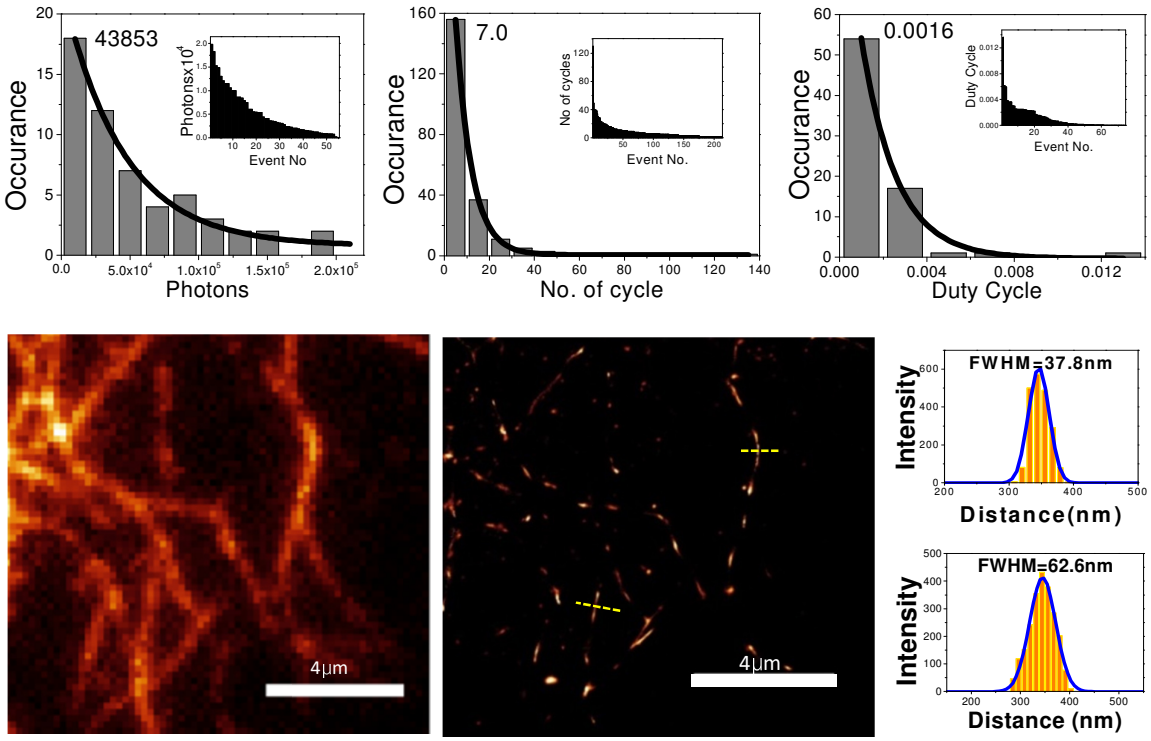

Figure S7. Top panel: Measured photon counts, on-off duty cycle and number of switching events of ATTO 647N. Bottom panel: TIRF image of actin filament stained with Phalloidin labelled ATTO-647N and its reconstructed image. The least filament thickness was observed as 38 nm from our measurement.

Table S1. Comparison of the photon counts, on-off duty cycle and number of switching cycles of CD alongwith the measured Cy3 and also with the reported dyes and fluorescent proteins.

S.N.	Fluorescent probe	Excitation Wavelength (nm)	Emission Wavelength (nm)	Photons counts	Number of switching cycles (mean)	On-off duty cycle
1	**CD (This work)**	532	570	2,986	4.2	0.0036
2	Cy3 Measured	532	570	8,774	1.8	0.0004
3	Cy3 Reported	550	570	8,158	1.6	0.0003
	Other dyes**					
4	Cy2	489	506	3,208	0.7	0.00045
5	Cy3B	559	570	2,057	5	0.0004
6	Day Light 750	752	778	749	6	0.0002
7	Cy7	747	776	997	2.6	0.0004
8	Alexa Fluor 750	749	775	703	6	0.0004
9	Alexa Flour 790	785	810	740	2.7	0.0014
	Fluorescent proteins ¥¥					
10	PAmcherry1	564	595	725	1	
11	Dronpa	503	518	120	60	
12	Dreiklang	511	529	700	-----	
13	MEos2	569	581	1000	2.8	
14	MEos3.2	572	580	1000	2.4	
15	mMaple	566	583	1000	3.4	
16	mMaple2	566	583	800	-----	

[a] ** taken from reference 7 in the main manuscript [b] ¥¥ taken from reference 24 in the main manuscript.

(1) Lin,Y.; Long, J. J.; Huang,F.; Duim,W. C. ; Kirschbaum, S.; Zhang, Y.; Schroeder, L. K.; Rebane, A. A.; Velasco, M. G. M et al Quantifying and Optimizing Single-Molecule Switching Nanoscopy at High Speeds. *PLoS One*, **2015**, *10(5)*, 0128135.

(2) Endesfelder, U.; Heilemann, M. Art and Artifacts in Single-Molecule Localization Microscopy: Beyond Attractive Images. *Nat. Meth.* **2014**, *11* (3), 235–238.

(3) Burgert, A; Letschert, S.; Doose, S.; Sauer, M. Artifacts in single-molecule localization microscopy. *Histochem Cell Biol*, **2015**, *144(2)*, 123-131.